Hindawi
Geofluids
Volume 2020, Article ID 8839333, 12 pages
https://doi.org/10.1155/2020/8839333

Research Article

Study on In Situ Stress Measurement and Surrounding Rock Control Technology in Deep Mine

Zhongcheng Qin,[1] Bin Cao,[1] Yongle Liu,[1] and Tan Li[2]

[1]*School of Mining and Safety Engineering, Shandong University of Science and Technology, Qingdao 266590, China*
[2]*Mining Research Institute, Inner Mongolia University of Science and Technology, Baotou 014010, China*

Correspondence should be addressed to Bin Cao; 18306483735@163.com

Received 6 August 2020; Revised 26 August 2020; Accepted 31 August 2020; Published 8 September 2020

Academic Editor: Zhijie Wen

In situ stress is the direct cause of roadway deformation and failure in the process of deep mining activities. The measured data of in situ stress in the Shuanghe coal mine show that the maximum principal stress is 44.94~50.61 MPa, and the maximum principal stress direction is near horizontal direction, which belongs to tectonic stress field. The maximum horizontal principal stress is 1.66~1.86 of the vertical stress. The horizontal principal stress controls the deep stress field. According to the measured data of in situ stress, the high-strength prestress bolt and cable collaborative support form is designed in the Shuanghe coal mine. Based on the stress field research of bolt and cable, the optimal prestress ratio of bolt and cable is proposed as 3. When the prestress ratio of bolt and cable is constant, the smaller the length ratio of bolt and cable is, the better the effect of prestressed field formed by cooperative support is. The results are applied to the support design of the mining roadway in the Shuanghe coal mine. Through the field monitoring test results, it is found that the maximum roof subsidence is 86 mm, the maximum floor deformation is 52 mm, and the maximum deformation of two sides is 125 mm. The surrounding rock control effect of the roadway is good, and the surrounding rock deformation conforms to the engineering technology standard requirements. The research results of this paper can provide some reference for the surrounding rock support of high ground stress mining roadway under similar conditions.

1. Introduction

In recent years, China's coal mining depth has increased year by year, especially in the central and eastern regions, the shallow coal resources have nearly exhausted, and the coal mines have entered the stage of deep mining. According to the statistics in 2019, only in Shandong Province, there are 16 mines with a depth of more than 1 km, accounting for 37.2% of China's mines with a depth of 1 km. Deep coal mining will face more complex mining environment, roadway deformation is large, floor heave and rib spalling are serious, and rock burst occurs from time to time. The traditional mining engineering design method based on experience analogy often leads to underground tunnel engineering instability and serious engineering accidents. Based on the existing research data, it is found that in situ stress is the main cause of roadway deformation and failure in deep mining activities of coal mine. The magnitude and direction of in situ stress have a significant impact on the stability of the surrounding rock of the roadway. By understanding the law of in situ stress, we can not only understand the original rock stress of roadway location but also provide basis for roadway support parameters [1–6].

Many scholars have done a lot of research on in situ stress measurement in coal mine and its influence on surrounding rock stress and failure. Wang et al., in order to study the causes of dynamic disasters and control technology in the Hongyang mining area, the stress relief method is used to measure the in situ stress at different buried depths. Through the combination of the measured results and numerical simulation, it is possible to predict the geological stress in a large range and provide a basis for engineering excavation [7]. Chen and Hua obtained the characteristics of high-level stress structure on the basis of 20 sets of in situ stress data

Name	Graphic	Depth (m)	Thick (m)	Lithology characterization
Midsand		1094.34	8.24	Light gray white, angular, local ferryginous nodule, RQD : 90%.
Mudstone		1095.32	0.98	Black, with neat fracture, containing a small amount of iron ore nodules, RQD : 40%
3 coal up		1097.42	2.10	Black, scale shape, mainly light coal, followed by dark coal.
Mudstone		1099.70	2.28	Black gray, a small amount of carbon, uneven fracture, RQD : 60%
Packsand		1103.00	3.30	Dark gray, neat fracture, containing a small amount of plant fossils, RQD : 60%
Mudstone		1106.30	3.30	Black gray, a small amount of carbon, uneven fracture, RQD : 70%
Packsand		1109.70	3.40	Gray, mainly compose of quartz, argillaceous calcium cementation, parallel bedding, RQD : 85%
Siltstone		1116.80	7.10	Gray, neat fracture
Packsand		1125.80	9.00	Gray, mainly composed of quartz, calcereous cementation, parallel bedding, with a small amount of pyride nodules, RQD : 90%
Siltstone		1128.40	2.60	Gray, neat fracture light gray, wave bedding containing a small amount of mica.
Packsand		1130.62	2.22	Gray, mainly composed of quartz, argillaceous calcium cementation, parallel bedding, RQD : 95%
3 coal down		1132.62	2.00	Black, scale shape, mainly light coal, followed by dark coal.
Mudstone		1134.24	1.62	Dark gray, regular fracture, containing a small number of plant rhizome fossils, RQD : 90%
Siltstone		1137.20	2.96	Dark gray, containing a small amount of pyrite nodules and plant rhizome fossils, RQD : 80%

Figure 1: The coal seam borehole histogram.

of 7 mines in the Huainan mining area. By studying the deformation of roadway under different lateral pressure coefficient at the measuring point, the best angle between roadway layout direction and maximum horizontal principal stress is obtained [8]. Cui et al. used the discrete element analysis method to study the stress distribution and failure characteristics of the surrounding rock loose zone of a rectangular roadway under different in situ stress characteristics. The results showed that the greater the stress difference value between the roof and the two sides of the rectangular roadway, the greater the depth and failure range of the surrounding rock loose zone of the rectangular roadway and further confirmed that the horizontal in situ stress is the main factor affecting the deformation and failure of the roadway, one of the factors [9]. Geng et al. aimed to support the problem of deep high-stress coal roadway, explored the failure characteristics of the roadway under different in situ stress and lateral pressure coefficient, and compared the support effect of the rectangular roadway and trapezoidal roadway under different support parameters, and pointed out that the optimization design of cross-section shape and reasonable support parameters are to improve the roadway support efficiency under the condition of deep high in situ stress key factors of fruit [10]. Jiang et al. applied in situ stress measurement data and three-dimensional modeling technology to study the vertical stress of coal pillar at different positions in the structural stress area, horizontal stress and the deformation of surrounding rock vary with the width of coal pillar, and

based on this, the reasonable width of the coal pillar along goaf in tectonic stress area was determined [11]. Liu et al. pointed out that the key factor to solve the deformation and instability of a roadway is to select a reasonable roadway section and layout method according to the characteristics of in situ stress distribution. Based on this, by studying the failure characteristics of the roadway under the conditions of different roadway cross-section forms, roadway strike, and maximum horizontal principal stress angle, it is concluded that the stability of the roadway is the best when the roadway section is straight wall semicircle arch and the roadway layout direction is parallel to the maximum horizontal principal stress [12].

The Shuanghe coal mine is a new mine in Shandong Province. The depth of the shaft is more than 1 km and the in situ stress is high. The Sanhejian coal mine, located in the shallow part of the Shuanghe coal mine, has experienced several large-scale rock burst accidents in the mining process, causing serious casualties and property losses. Therefore, if the design of roadway support form in the Shuanghe coal mine is not reasonable, the roadway support will be extremely difficult and cannot meet the needs of a safe and efficient mining. Taking the first coal working face of the Shuanghe coal mine as the research background, based on the field measured data of in situ stress, through theoretical analysis, numerical simulation, and field measurement methods, this paper studies the effect of bolt and cable collaborative support technology in deep mine high in situ stress mining roadway. The results of this paper can provide reference for the development of deep mining roadway support research and ensure the safety of coal mine production.

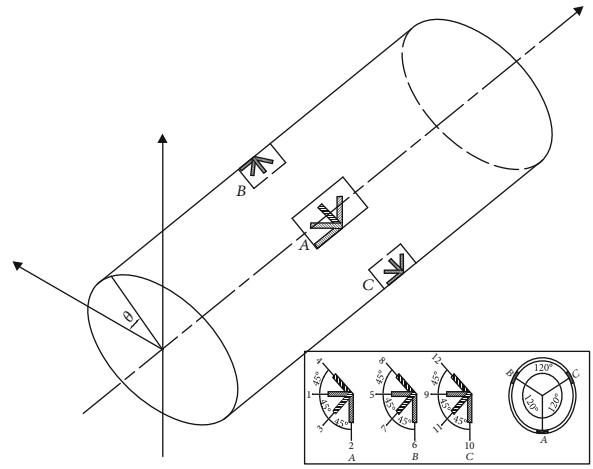

Figure 2: Strain gauge distribution of CSIRO.

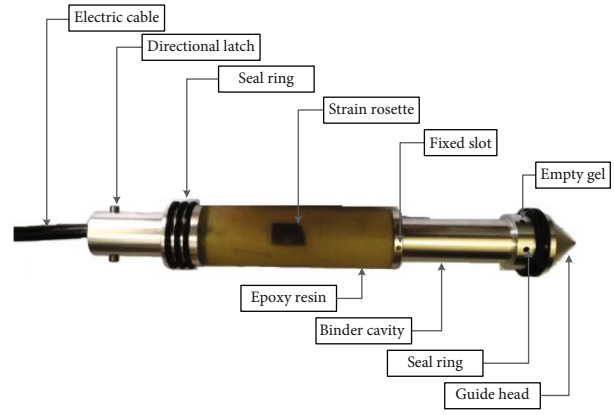

Figure 3: Structural diagram of CSIRO.

2. Engineering Geological Description

The Shuanghe coal mine is located in the juncture of Shandong Province and Jiangsu Province, and its administrative area belongs to Yutai County, about 10 km away from the urban area of Yutai County. The coal seam in the mine field is deeply buried, and the occurrence elevation of the coal seam is between -750 and approximately -1200 m. The initial mining coal seam is relatively shallow, with a buried depth of 800~1100 m. The coal seam is relatively stable with a gentle dip angle of 12° on average. The thickness of 3_{upper} coal seam is 1.25~3.10 m with an average thickness of 2.08 m. The roof is mainly composed of mudstone and siltstone, which belongs to medium stability roof, and the lithology of floor is mainly siltstone. The thickness of 3_{down} coal seam is 2.00~3.64 m, and the average thickness is 2.98 m. The roof is medium fine sandstone, which is stable roof, and the floor is siltstone. The coal seam borehole histogram is shown in Figure 1.

In April 2019, Shandong Coal Mine Safety Supervision Bureau and Shandong Provincial Energy Bureau determined 41 rock burst mines and 20 mines with a depth of more than 1000 meters in Shandong Province, among which Shuanghe coal mine is listed. Shuanghe coal mine coal seam roof and floor rock strength is high and is medium hard to hard rock, respectively, the rock layer thickness is large, and the geological structure is located in Tengxian anticline dip end, turning end. Due to the deep buried coal seam, high self-weight stress and complex geological structure, the late mining process is faced with serious rock burst threat and roadway surrounding rock control problems. Based on this, in September 2019, the person in charge of the coal mine entrusted the research group of the author to enter the site to measure the in situ stress of the Shuanghe coal mine and guide the roadway support.

3. In Situ Stress Measurement Process and Result Analysis

In 2003, the International Association of Rock Mechanics and Engineering recommended the use of hydraulic fracturing method and stress relief method for in situ stress measurement. As one of the more mature and commonly used methods in in situ stress testing, the hollow inclusion strain gauge stress relief method has the advantages of simple operation, obtaining all components of the stress field tensor at one time, and has been widely used in the in situ stress measurement of deep mines in China [13–18].

Table 1: Drilling design parameters of each measuring point.

Survey point number	Drilling position	Underground depth (m)	Actual drilling parameters			
			Large diameter drilling depth (m)	Small diameter drilling depth (m)	Azimuth (°)	Dip (°)
Point no. 1	Chamber for water exploration in the parking lot at the bottom of the first mining area	1085	10	0.4	60	10.5
Point no. 2	In the roadway leading to the auxiliary shaft near the pit bottom parking lot	1089	12	0.4	60	10
Point no. 3	In the tunnel leading to the sump	1089	12	0.4	60	10.5

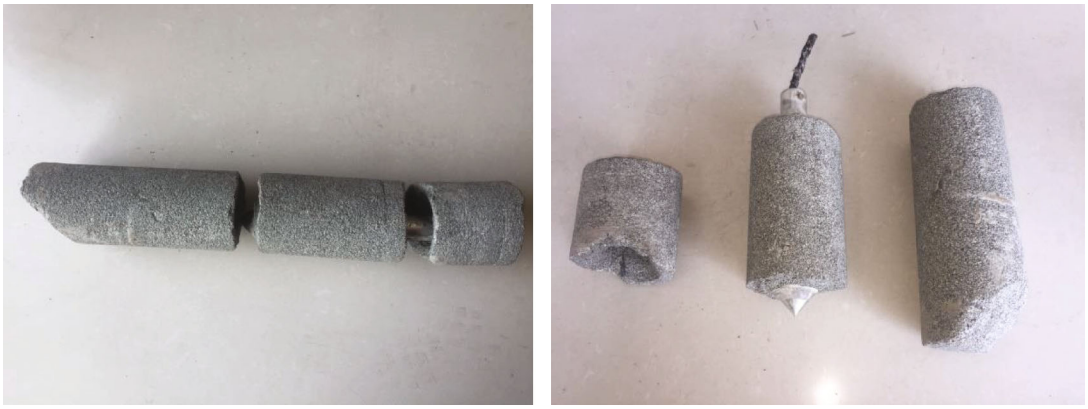

Figure 4: Core samples from some survey points.

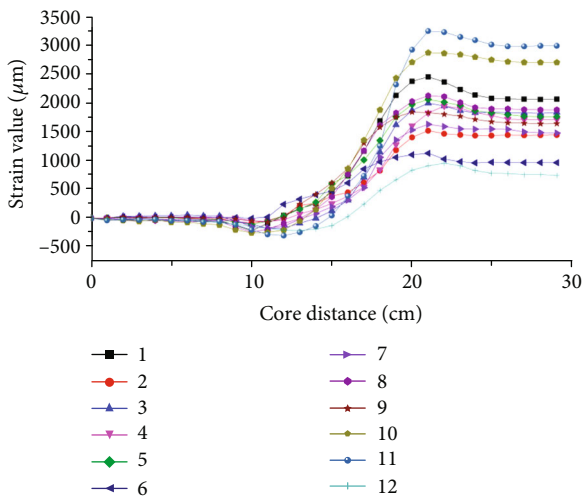

Figure 5: Stress relief curve of no. 1 measuring point.

KX-81 CSIRO developed by the Institute of Geomechanics of Chinese Academy of Sciences is used in the Shuanghe coal mine. The hollow inclusion strain gauge has a total length of 260 mm and a diameter of 36 mm. Its main components are three groups of strain flowers embedded in epoxy resin at 120° intervals along the circumference. Each group of strain flowers is composed of four strain gauges, which are arranged 45° apart along the cylinder wall of a hollow inclusion strain gauge collect strain values in different directions. The strain rosette distribution of KX-81 CSIRO is shown in Figure 2. Each hollow inclusion strain gauge has 14 wires, including 12 strain gauge connections, 1 ground wire, and 1 compensation wire. The structure of the CSIRO is shown in Figure 3.

3.1. Arrangement of In Situ Stress Measuring Points. Underground in situ stress measurement is easily affected by the mining work, which leads to the error of in situ stress measurement results. In order to ensure the accuracy of the measurement results, the layout of in situ stress measuring points should meet the following principles:

(1) Select representative areas. Avoid stress change area, unstable area, and interference source

(2) In the rock mass which is complete or complete as far as possible, the joints and fissures are not developed or well cemented, except for special requirements, they are generally far away from faults and away from rock fracture zones and fracture development zones

(3) Far away from or as far as possible away from the larger excavation body, such as large goaf and large chamber

(4) Avoid the stress concentration area of roadway and stope and ensure that the stress measuring point must be located in the original rock stress area, that is, the section where the stress state is not disturbed by the project

According to the selection principle of in situ stress measuring points, combined with the geological conditions and roadway layout conditions of the Shuanghe coal mine, the

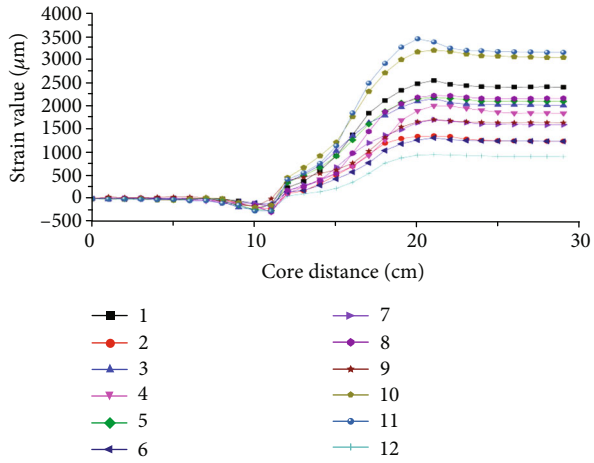

Figure 6: Stress relief curve of no. 2 measuring point.

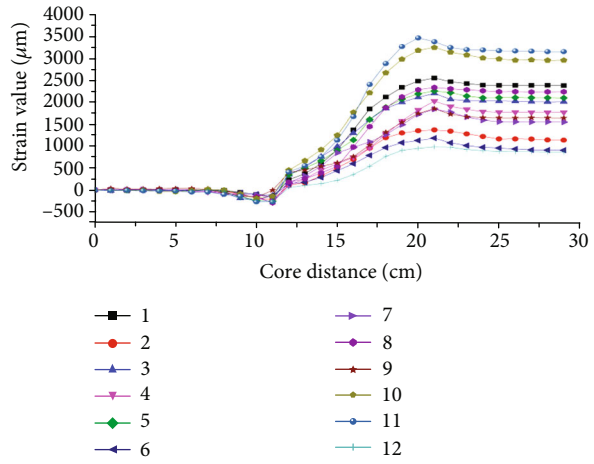

Figure 7: Stress relief curve of no. 3 measuring point.

Table 2: Rock mechanical parameters of core at each measuring point.

Survey point number	Modulus of elasticity (GPa)	Poisson's ratio
Point no. 1	18.4	0.19
Point no. 2	19	0.21
Point no. 3	19	0.21

location of this in situ stress measuring point is determined through the field survey and analysis of the underground. See Table 1 for parameters of each measuring point.

3.2. Stress Relief and Data Solution. By using the method of CSIRO to test the in situ stress of the Shuanghe coal mine, in the process of core extraction, the CSIRO will change correspondingly with the elastic recovery of the rock mass. In this process, the mine intrinsic safety strain acquisition instrument records the data changes of each strain gauge. Some of the cores collected on site are shown in Figure 4, and the stress relief curve of three measuring points is shown in Figures 5–7.

In the process of core extraction, the relationship between the in situ stress and the measured strain can be expressed by the following formula [19–30]:

$$\varepsilon_{90^\circ} = \frac{1}{E}\left\{\left(\sigma_x + \sigma_y\right)k_1 + 2\left(1-\mu^2\right) \cdot \left[\left(\sigma_y - \sigma_x\right)\cos 2\theta - 2\tau_{xy}\sin 2\theta\right]k_2 - \mu\sigma_z k_4\right\}, \tag{1}$$

$$\varepsilon_0 = \frac{1}{E}\left[\sigma_z - \mu\left(\sigma_x - \sigma_y\right)\right], \tag{2}$$

$$\gamma = k_3\frac{4}{E}(1+\mu)\left(\tau_{yz}\cos\theta - \tau_{xz}\sin\theta\right), \tag{3}$$

$$\varepsilon_{\pm 45^\circ} = \frac{\left(\varepsilon_{90^\circ} + \varepsilon_0 + \gamma\right)}{2}, \tag{4}$$

where ε_{90° represents the circumferential strain value measured by the CSIRO; ε_0 represents the axial strain value measured by the CSIRO; $\varepsilon_{\pm 45^\circ}$ represents the strain value measured by the CSIRO in the positive and negative 45°directions; γ represents the shear strain value measured by the CSIRO; E represents the elastic modulus; μ represents Poisson's ratio; σ_x, σ_y, σ_z, τ_{xy}, τ_{yz}, and τ_{zx}, respectively, represents the three-dimensional stress component at the measuring point; and k_1, k_1, k_1, and k_1 denotes the correction factors added by Vorotniki and Walton, respectively.

According to the relationship between three-dimensional stress components the values of σ_x, σ_y, σ_z, τ_{xy}, τ_{yz}, and τ_{zx} at any point can be expressed by

$$\sigma_x = \frac{B(c_1+c_2) - 2Ac_3}{4\left(BX - A^2\right)} + \frac{c_1 - c_2}{4Y}, \tag{5}$$

$$\sigma_y = \frac{B(c_1+c_2) - 2Ac_3}{4\left(BX - A^2\right)} - \frac{c_1 - c_2}{4Y}, \tag{6}$$

$$\sigma_z = \frac{-2A(c_1+c_2) + 4Xc_3}{4\left(BX - A^2\right)}, \tag{7}$$

$$\tau_{xy} = \frac{\sqrt{3}E\left(2\varepsilon_5' + \varepsilon_7' + \varepsilon_8' - 2\varepsilon_9' - \varepsilon_{11}' - \varepsilon_{12}'\right)}{36k_3\left(1-\mu^2\right)}, \tag{8}$$

$$\tau_{yz} = \frac{\sqrt{3}E\left(\varepsilon_7' - \varepsilon_8' - \varepsilon_{11}' + \varepsilon_{12}'\right)}{12k_3(1+\mu)}, \tag{9}$$

$$\tau_{zx} = \frac{E\left(2\varepsilon_3' - 2\varepsilon_4' - \varepsilon_7' + \varepsilon_8' - \varepsilon_{11}' + \varepsilon_{12}'\right)}{12k_3(1+\mu)}, \tag{10}$$

$$A = -3\mu(k_1k_4 + 1) + \frac{3(k_1-\mu)(1-\mu k_4)}{2}, \tag{11}$$

$$B = 3\mu\left(\mu^2k_4^2 + 1\right) + \frac{2\left(1-\mu k_4\right)^2}{2}, \tag{12}$$

$$X = 3k_1^2 + 3\mu^2 + \frac{2\left(k_1-\mu\right)^2}{2}, \tag{13}$$

$$Y = 9k_2^2\left(1-\mu^2\right)^2, \tag{14}$$

$$\begin{aligned} c_1 + c_2 = E\Big[&2k_1\left(\varepsilon_1' + \varepsilon_3' + \varepsilon_5'\right) - 2\mu\left(\varepsilon_2' + \varepsilon_6' + \varepsilon_{10}'\right) \\ &+ (k_1 - \mu)\left(\varepsilon_3' + \varepsilon_4' + \varepsilon_7' + \varepsilon_8' + \varepsilon_{11}' + \varepsilon_{12}'\right)\Big], \end{aligned} \tag{15}$$

$$c_1 - c_2 = Ek_2\left[(1-\mu)^2\left(4\varepsilon_1' + 2\varepsilon_3' + 2\varepsilon_4' - 2\varepsilon_5' - \varepsilon_7' - \varepsilon_8' - 2\varepsilon_9' - \varepsilon_{11}' - \varepsilon_{12}'\right)\right], \tag{16}$$

$$\begin{aligned} c_3 = -E\Big[&\mu k_4\left(\varepsilon_1' + \varepsilon_3' + \varepsilon_5'\right) - \left(\varepsilon_2' + \varepsilon_6' + \varepsilon_{10}'\right) + \frac{(1-\mu k_4)}{2} \\ &\cdot \left(\varepsilon_3' + \varepsilon_4' + \varepsilon_7' + \varepsilon_8' + \varepsilon_{11}' + \varepsilon_{12}'\right)\Big], \end{aligned} \tag{17}$$

where $\varepsilon_1', \varepsilon_2', \ldots\ldots\varepsilon_{11}', \varepsilon_{12}'$ represents the measured strain value of CSIRO.

For the core containing the CSIRO taken out on site, the confining pressure calibration test shall be carried out to obtain the elastic modulus and Poisson's ratio of the rock sample. The rock mechanical parameters of three measuring points obtained by confining pressure calibration test are shown in Table 2.

We input the strain data collected from the three measuring points and the surrounding rock mechanical parameters obtained from the core confining pressure calibration test into the professional in situ stress calculation software to solve the size and direction of the main stress of each test borehole, and the results are shown in Table 3.

3.3. Analysis of In Situ Stress Measurement Results. According to the above in situ stress test results, it can be seen that the in situ stress of the Shuanghe coal mine has the following laws.

Among the three in situ stress measuring points arranged underground in the Shuanghe coal mine, the maximum principal stress is 44.94~50.61 MPa, the maximum principal stress azimuth angle is 244.97°~245.98°, the maximum principal stress dip angle is 4.26°~5.11°, and the maximum principal stress direction is near horizonta; it belongs to the tectonic stress field.

With the increase of depth, the values of the maximum principal stress, the middle principal stress, and the minimum principal stress all show an upward trend, but the relative errors of dip angle and direction are all within 10%. The in situ stress test data of the Shuanghe coal mine are plotted into a scatter plot, and the relationship between in situ stress and buried depth is fitted, as shown in Figure 8. Using the least square method to deal with the measured data of in situ stress, the relationship formula between in situ stress and buried depth in Shuanghe coal mine is obtained as shown in equations (18)–(20).

Relationship between maximum principal stress and buried depth:

$$\sigma_{\max} = 1.3512H - 1421.17. \tag{18}$$

Relationship between minimum principal stress and buried depth:

$$\sigma_{\min} = 0.475H - 494.61. \tag{19}$$

Relationship between intermediate principal stress and buried depth:

$$\sigma_{\text{Intermediate}} = 0.6412H - 671.18. \tag{20}$$

The measured maximum horizontal principal stress is 2.16~2.28 times of the minimum horizontal principal stress, and the stress imbalance coefficient is high. The horizontal stress will have a more obvious directional effect on the excavation of the mining roadway. The layout of the mining roadway should be parallel to the direction of the maximum principal stress as far as possible, so as to reduce the deformation and failure of the surrounding rock of the roadway.

The measured maximum horizontal stress is greater than the vertical stress, and the maximum horizontal principal stress is 1.66~1.86 times of the vertical stress. The variation of lateral pressure coefficient with depth is not very obvious, and the overall distribution is about 1.34. Combined with the mining depth of the Shuanghe coal mine and the mechanical properties of coal and rock mass, it can be seen that the coal and rock mass under the Shuanghe coal mine are in high-stress state, and the deformation and failure of underground strata and the behavior law of mine pressure will be affected obviously affected.

4. Study on Support Technology of High-Stress Mining Roadway in Deep Mine

4.1. Study on Stress Field of Bolt and Cable Support. Bolt support is the main means of surrounding rock control in a coal mine roadway, which has solved a lot of practical problems in the engineering field. The prestress of bolt and cable and the length of bolt and cable are the decisive factors of bolt-cable cooperative supporting system. The prestress determines whether the bolt support form is active support or passive support. Larger prestress and appropriate length of bolt and cable can enhance the control effect of surrounding rock, restrain the separation of roadway roof, and improve the stability of the surrounding rock [31–40].

In order to study the distribution characteristics of supporting stress field produced by prestress bolt and cable and the effect of bolt-cable coupling support, FLAC numerical simulation method is applied to analyze the stress field of the bolt and cable support under different support conditions. Based on the theory of bolt and cable collaborative support, the optimal length ratio of bolt to cable and the prestress ratio of bolt to cable are studied, so as to select reasonable parameters of bolt and cable for later stage provides the basis. The first working face of the Shuanghe coal mine is selected as the simulation object. The cross-section of the roadway is rectangular, the width of the roadway is 3.6 m, and the height is 2.6 m. The two sides of the roadway are coal seams, the direct roof is thin mudstone, the thickness is 0.9 m, and the basic roof is medium sandstone. Boundary

Table 3: In situ stress measurement results of each measuring point.

Survey point number	Main stress type	Measured value (MPa)	Azimuth (°)	Dip angle (°)	σ_V	σ_x/σ_V	$\sigma_{max}/\sigma_{min}$
Point no. 1	σ_1	44.94	245.98	5.11	27.13	1.66	2.16
	σ_2	24.58	-24.88	-9.53		0.91	
	σ_3	20.77	183.84	-79.17		0.77	
Point no. 2	σ_1	50.08	244.97	4.58	27.23	1.84	2.28
	σ_2	26.76	-25.93	-11.03		0.98	
	σ_3	21.99	177.15	-78.03		0.81	
Point no. 3	σ_1	50.61	245.03	4.26	27.23	1.86	2.17
	σ_2	27.53	-26.10	-14.81		1.01	
	σ_3	23.35	170.67	-74.55		0.86	

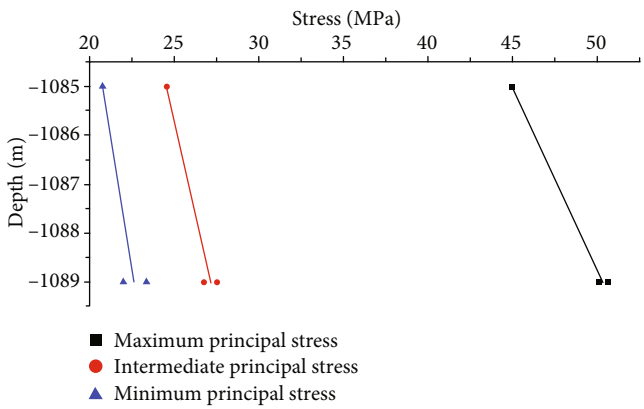

Figure 8: Relationship between in situ stress and buried depth.

conditions of numerical calculation are as follows: limit the top, bottom, and lateral displacement of the model, establish the model length × width × height as 60 m × 60 m × 60 m, see Table 4 for rock parameters of roadway roof and floor, and adopt a Mohr-Voulomb failure criterion, and do not consider coal seam dip angle here.

According to the orthogonal test method, under the premise of considering the horizontal uniformity and collocation uniformity, the three factors of anchor bolt preload, anchor cable length, and anchor cable preload are listed into the orthogonal test table. Each test takes six levels, and 36 groups of simulation experiments are carried out according to the orthogonal planning table (Table 5).

The cloud chart of the stress field generated by the support under the conditions of different bolt and cable support parameters is shown in Figure 9.

It can be seen from the above figure that the effective compressive stress zone is formed in the surrounding rock mass of the roadway after the bolt and cable are applied with preload. Under the comprehensive action of the bolt and cable prestress, the vertical stress at the roadway roof forms an inverted arch structure with a certain thickness and strength. Therefore, the prestress bolt and cable can exert an active constraint on the surrounding rock before the roadway deformation, so that the surrounding rock can recover the three-dimensional stress state, which plays an important role in increasing the bearing capacity of the surrounding rock and improving the supporting effect of roadway.

When the ratio of the bolt length to cable length is constant and the ratio of bolt stress to cable stress is small, the prestress of the cable plays a dominant role in the stress field formed by the interaction between bolt and cable, and the stress concentration area is mainly near the cable unit. At this time, the stress of the cable is larger, while the stress of the bolt is smaller. With the increase of bolt prestress, in the stress field formed by the interaction between bolt and cable, the stress concentration range is dispersed from the periphery of cable to the periphery of bolt, and the stress field formed by bolt and cable prestress is more balanced. By comparing the characteristics of the prestressed field formed by many schemes, it is concluded that, when the ratio of the prestress of the bolt and the cable is 3, the equilibrium degree of the prestressed field formed by the interaction between the bolt and the cable is the best.

When the ratio of bolt prestress to cable prestress remains unchanged and the length of cable increases, in the same range of stress field, the stress value decreases, which indicates that when the prestress is constant, the length of cable increases, and the control effect of cable on surrounding rock of roadway decreases. In order to improve the supporting effect of cable by adding prestress, the limit of the yield strength of the cable should be considered. When the prestress of the cable remains unchanged, the support effect of the short cable on the surrounding rock of the roadway is better. According to the suspension theory, the main function of the cable is to suspend the unstable rock layer at the lower part of the roof to the stable rock layer above. Therefore, when the bolt length and cable length meet the suspension requirements, the ratio of bolt length to anchor cable length should be as small as possible to enhance the control effect of the collaborative support system on the surrounding rock of the roadway.

4.2. Surrounding Rock Control Technology of High-Stress Mining Roadway in Deep Mine. Based on the above study, it can be seen that the reasonable parameters of bolt and cable cooperative support play an important role in the control of

Table 4: Physical and mechanical parameters of rock.

Number	Rock properties	Shear modulus (GPa)	Bulk modulus (GPa)	Cohesion (MPa)	Tensile strength (MPa)	Internal friction angle (°)	Density (kg·m^3)
1	Sandstone	1.6	2.7	2.1	1.6	38	2540
2	Medium sandstone	2.5	3.3	4.0	2.2	37	2580
3	Mudstone	1.5	1.7	1.8	1.4	39	2768
4	Coal	0.5	1.0	1.2	0.6	35	1450
5	Siltstone	3.6	4.3	7.1	10.2	33	2740

Table 5: Orthogonal programming table.

Number	Bolt pretension	Length of anchor cable	Pretightening force of anchor cable	Number	Bolt pretension	Length of anchor cable	Pretightening force of anchor cable
1	20	3.6	50	19	80	3.6	200
2	20	4.8	100	20	80	4.8	250
3	20	6.0	150	21	80	6.0	300
4	20	7.2	200	22	80	7.2	50
5	20	8.4	250	23	80	8.4	100
6	20	9.6	300	24	80	9.6	150
7	40	3.6	100	25	100	3.6	250
8	40	4.8	150	26	100	4.8	300
9	40	6.0	200	27	100	6.0	50
10	40	7.2	250	28	100	7.2	100
11	40	8.4	300	29	100	8.4	150
12	40	9.6	50	30	100	9.6	200
13	60	3.6	150	31	120	3.6	300
14	60	4.8	200	32	120	4.8	50
15	60	6.0	250	33	120	6.0	100
16	60	7.2	300	34	120	7.2	150
17	60	8.4	50	35	120	8.4	200
18	60	9.6	100	36	120	9.6	250

surrounding rock of roadway. In this section, the high-strength prestress bolt and cable collaborative support technology is applied to the 3_{upper}-101 first mining face of the Shuanghe coal mine. In order to compare the support effect of high-strength prestress bolt and cable on the surrounding rock of the roadway, two support schemes of ordinary bolt and cable cooperative support and high-strength prestress bolt and cable cooperative support are established. The model size is 60 m × 60 m × 60 m, and the roadway size is 3.6 m × 2.6 m. The stress boundary conditions are applied around the model according to the average value of measured in situ stress in the Shuanghe coal mine, and the boundary displacement of the model is controlled. The numerical model is shown in Figure 10.

Figures 11–14 show the comparison of surrounding rock control effect under different bolt and cable cooperative support forms. It can be seen from the figure that the control effect of the surrounding rock of the roadway is obvious when the high-strength prestress bolt and cable cooperative support are adopted.

5. Engineering Application Effect Inspection

In the Shuanghe coal mine, the cross-section of track gateway in 3_{upper}-101 working face is rectangular, with a roadway height of 2.6 m and width of 3.6 m. The roof is supported by high-strength prestress bolt, high-strength prestress cable, metal mesh, and steel belt. The bolt specification is $\Phi 22 \times 2400$ mm. The prestress moment is 350 KN·m. The row spacing is 800 × 800 mm. The cable specification is $\Phi 21.8 \times 4000$ mm. The prestress is 240 KN·m. The row spacing is 1600 × 1600 mm. Two sides of the roadway are supported by high-strength prestress bolt. The bolt specification is $\Phi 22 \times 2400$ mm. The prestress moment is 350 KN·m. The row spacing is 800 × 800 mm. The specific support scheme is shown in Figure 15.

After the implementation of the support scheme, the deformation of surrounding rock and the stress of bolt and cable were observed for 60 days. The monitoring results are shown in Figures 15–18.

It can be concluded from the above figure that the deformation of the roadway surrounding rock can be effectively

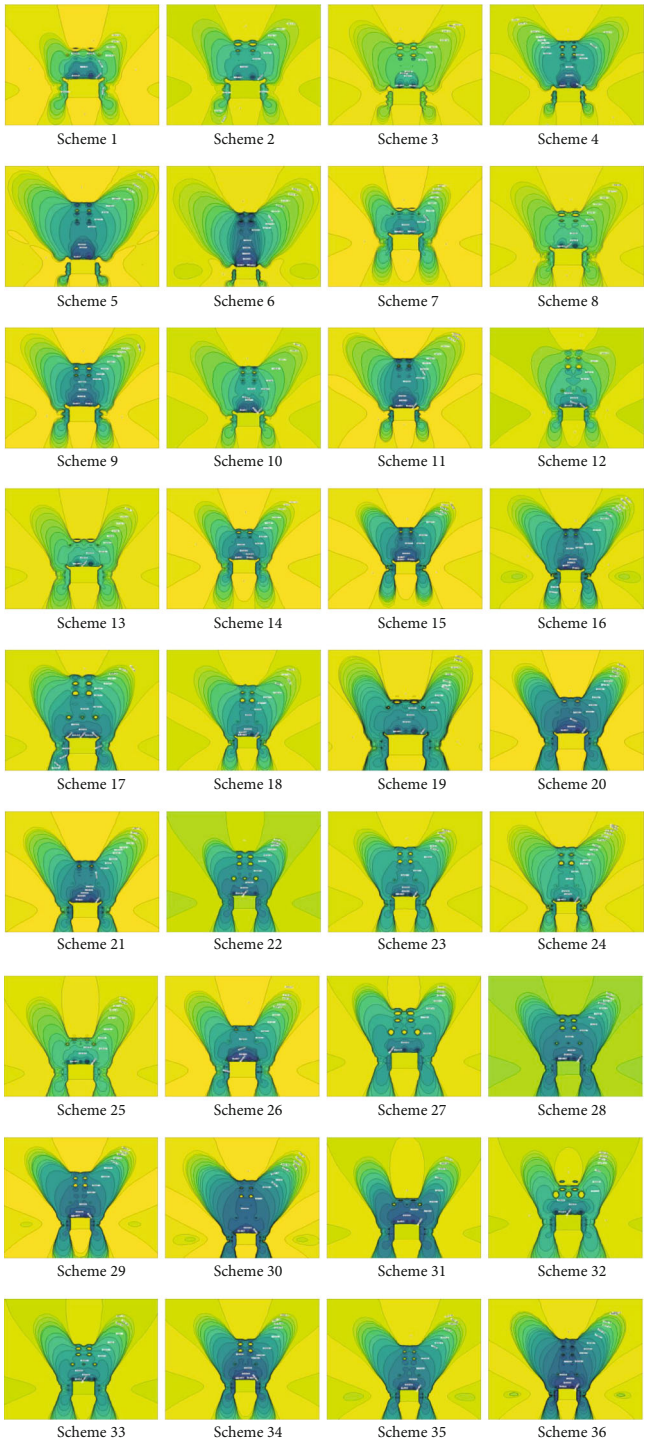

Figure 9: Stress field cloud chart of different support schemes.

controlled after using high-strength prstress bolt and cable collaborative support. Based on the observation results of 60 days, the maximum roof subsidence is 86 mm, the maximum floor deformation is 52 mm, and the maximum deformation of two sides is 125 mm. The deformation of the surrounding rock of the roadway meets the relevant requirements of coal mine operation regulations. In addition, due to the application of prestress, the stress of the bolt and cable is

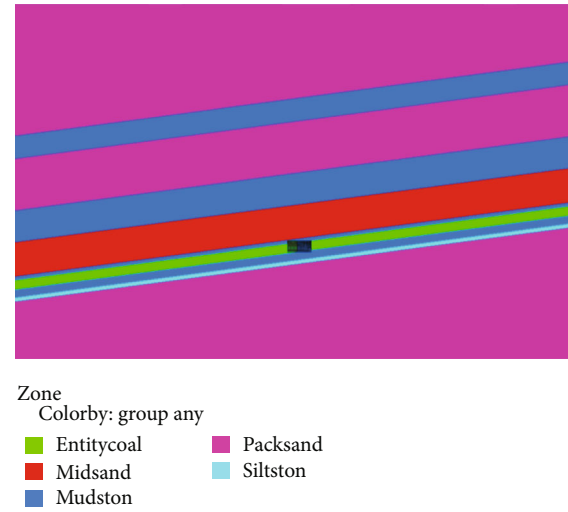

Figure 10: The numerical model.

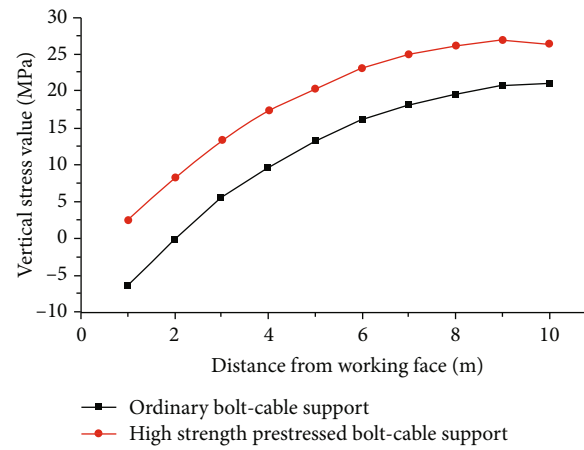

Figure 11: Vertical stress of the roof.

generally large. The maximum stress value of the bolt is 83 KN, and the maximum stress value of cable is 256 KN. The stress of the bolt and cable does not decrease. The results show that the effect of the bolt and cable cooperative support technology on roadway control is better.

6. Conclusion

(1) The magnitude and direction of in situ stress have a great influence on the stability of the surrounding rock of the roadway. The measured maximum principal stress in the Shuanghe coal mine is 44.94~50.61 MPa, and the dip angle of the maximum principal stress is between 4.26° and approximately 5.11°. The direction of the maximum principal stress is near horizontal direction, and the three measuring points are dominated by horizontal force. The maximum horizontal principal stress is 2.16~2.28 times of the minimum horizontal principal stress, and the stress disequilibrium coefficient is high. The

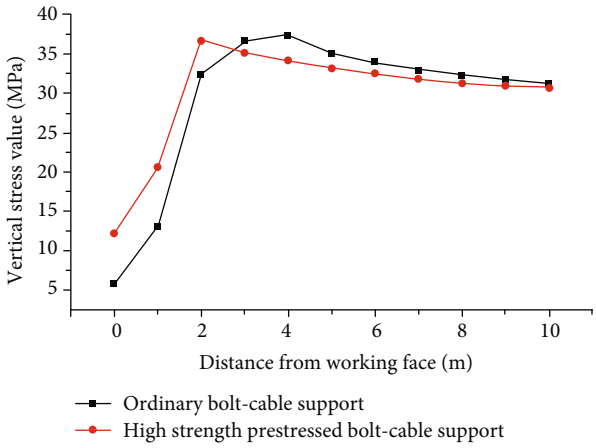

Figure 12: Vertical stress of two sides.

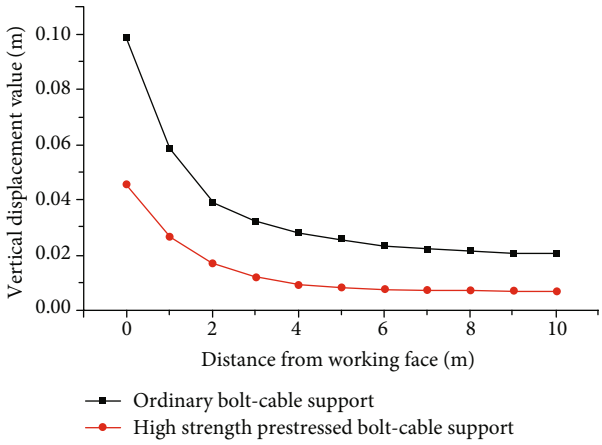

Figure 13: Vertical displacement of the roof.

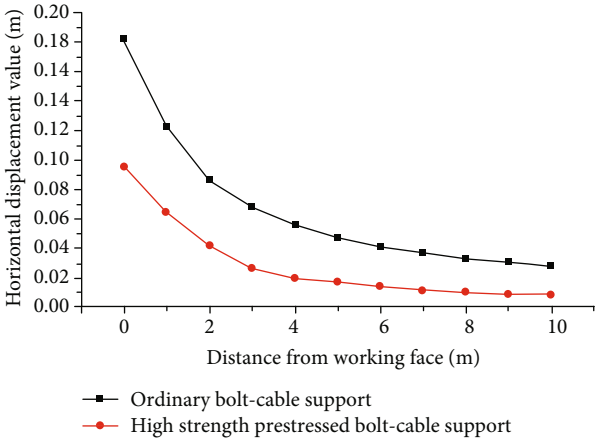

Figure 14: Horizontal displacement of two sides.

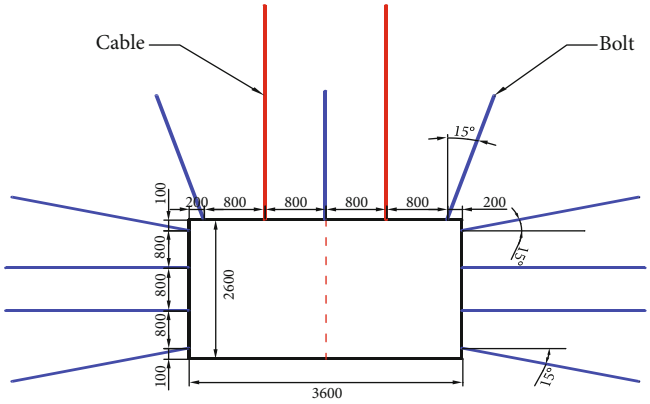

Figure 15: Roadway support scheme.

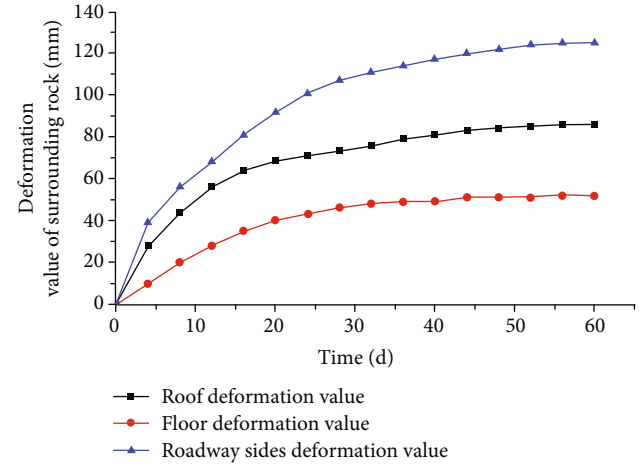

Figure 16: Deformation value of the roadway surrounding rock.

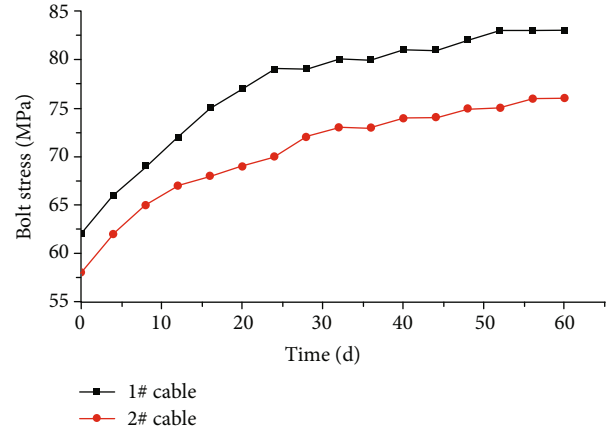

Figure 17: Stress condition of the bolt.

maximum horizontal principal stress is 1.66~1.86 times of the vertical stress, and the lateral pressure coefficient changes little, fluctuating around 1.34

(2) Through the research of FLAC numerical simulation software, it is found that, when the prestress of bolt and cable is determined, the smaller the ratio of bolt length to cable length is, the more stable the prestressed field is. When the length of cable is determined, the stability of the prestressed field is the best when the ratio of prestress of bolt and cable is 3

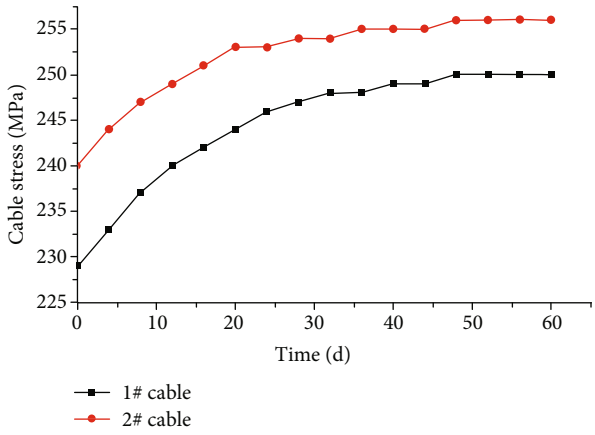

Figure 18: Stress condition of the anchor cable.

(3) The mining roadway of the Shuanghe coal mine adopts the high-strength prestress bolt and cable collaborative support technology. After 60 days of continuous ground pressure observation results, the maximum roof subsidence is 86 mm, the maximum floor deformation is 52 mm, the maximum deformation of two sides is 125 mm, the maximum stress value of bolt is 83 KN, the maximum stress value of anchor cable is 256 KN, and the stress of bolt and cable does not decline. The deformation of roadway surrounding rock meets the relevant requirements of coal mine operation regulations, and the effect of surrounding rock control is significant

Data Availability

The authors declare that all data supporting the findings of this study are available within the article, the reader can find and use it; there is no unavailable date.

Conflicts of Interest

The authors declare that there are no conflicts of interests regarding the publication of this paper.

Acknowledgments

This paper was supported by the National Natural Science Foundation of China (51379119, 51304126, and 51109124).

References

[1] H. P. Kang, L. P. Si, and X. Zhang, "Characteristics of underground in-situ stress distribution in shallow coal mines and its applications," *Journal of China Coal Society*, vol. 41, no. 6, pp. 1332–1340, 2016.

[2] C. H. Wang, "Brief review and outlook of main estimate and measurement methods for in-situ stresses in rock mass," *Geological Review*, vol. 60, no. 5, pp. 971–996, 2014.

[3] Z. L. Wang, H. P. Kang, and J. Lin, "Study on structural stress of fold zone affected to mine roadway support," *Coal Science and Technology*, vol. 39, no. 5, pp. 25–28, 2011.

[4] Y. X. Zhao, Y. D. Jiang, and K. X. Zhang, "Analysis of gate road stability in underground coal mining based on disturbed state theory," *Journal of China University of Mining & Technology*, vol. 43, no. 2, pp. 233–240, 2014.

[5] C. Y. Zhang, M. L. Wu, and C. T. Liao, "In- situ stress measurement and study of stress state characteristics of Jinchuan No. 3 mine," *Rock and Soil Mechanics*, vol. 34, no. 11, pp. 3254–3260, 2013.

[6] H. P. Kang, J. Lin, X. Zhang, and Y. Z. Wu, "In-situ stress measurements and distribution laws in Lu'an underground coal mines," *Rock and Soil Mechanics*, vol. 31, no. 3, pp. 827–831, 2010.

[7] J. Wang, Z. H. Feng, Z. G. Meng, Y. L. Zhang, and H. Wang, "In situ stress measurement and numerical analysis of Hongyang mining area," *Journal of Mining & Safety Engineering*, vol. 34, no. 1, pp. 134–140, 2017.

[8] D. H. Chen and X. Z. Hua, "The deformation law of the sur-rounding rock in deep mining roadways under the influence ofmulti-factors and the control counter measures," *Journal of Mining & Safety Engineering*, vol. 34, no. 4, pp. 760–768, 2017.

[9] L. W. Cui, S. S. Yang, and X. J. Tong, "Study on the influence of in-situ stress characteristics on deformation of surrounding rock loose zone in rectangular roadway," *Mining Research and Development*, vol. 36, no. 1, pp. 80–83, 2016.

[10] J. Y. Geng, F. T. Wang, Y. Zhang, J. G. Ban, and G. Li, "Research on key technology of surrounding rock control in high stress coal roadway," *Coal Science and Technology*, vol. 47, no. 9, pp. 189–196, 2019.

[11] Y. D. Jiang, H. H. Song, Z. Q. Ma, B. J. Ma, and L. T. Gao, "Optimization of narrow coal pillar width of gob side entry in tectonic stress area based on in-situ stress inversion," *Journal of China Coal Society*, vol. 43, no. 2, pp. 319–326, 2018.

[12] C. Liu, Y. X. Li, and M. Tan, "Research on roadway stability optimization based on 3D in-situ stress measurement," *Chinese Journal of Underground Space and Engineering*, vol. 14, no. 5, pp. 1372–1380, 2018.

[13] B. H. Zhang, L. J. Han, G. L. Han, and Y. N. Wang, "Study of 3D in-situ stress measurement and stability of roadways in depth," *Rock and Soil Mechanics*, vol. 29, no. 9, pp. 2547–2550, 2008.

[14] Q. Fu, Y. C. Zhao, D. X. He, D. F. Lu, and Y. B. Zhen, "Impact of roadway shape on high stress soft rock roadway deformation," *Safety in Coal Mines*, vol. 45, no. 9, pp. 197–199, 2014.

[15] C. Wang, S. H. Tu, Z. X. Li, Q. S. Bai, and H. S. Tu, "Section optimization of deep gateways in three soft coal seam," *Journal of China University of Mining & Technology*, vol. 44, no. 1, pp. 9–15, 2015.

[16] W. J. Wang, C. Yuan, W. J. Yu, H. Wu, and W. Q. Peng, "Stability control method of surrounding rock in deep roadway with large deformation," *Journal of China Coal Society*, vol. 41, no. 12, pp. 2921–2931, 2016.

[17] W. J. Wang, C. Yuan, W. J. Yu, H. Wu, and W. Q. Peng, "Control technology of reserved surrounding rock deformation in deep roadway under high stress," *Journal of China Coal Society*, vol. 41, no. 9, pp. 2156–2164, 2016.

[18] H. Y. Du, Y. L. Si, C. Y. Li, and W. S. Wei, "Study on roof failure characteristics of roadway under nonuniform stress," *Coal Science and Technology*, vol. 47, no. 5, pp. 101–106, 2019.

[19] F. Q. Gao, "Numerical analysis of the influence of the maximum horizontal principal stress on the stability of

surrounding rock," *Mining Research and Development*, vol. 1, pp. 62–64, 2008.

[20] G. M. Li, C. Zhou, and X. D. Wang, "Research on influence of the maximum principal stress direction on stability of roadway surrounding rock," *Industry and Mine Automation*, vol. 45, no. 10, pp. 38–42+73, 2019.

[21] X. N. Chen, P. Shen, X. Y. Xiong, and J. W. Fan, "Experimental study on the unsymmetrical characteristics of surrounding rock stress of right angle trapezoid roadway in inclined coal seam," *Coal Technology*, vol. 38, no. 1, pp. 13–15, 2019.

[22] Z. J. Wen, E. R. Xing, and S. S. Shi, "Overlying strata structural modeling and support applicability analysis for large mining-height stopes," *Journal of Loss Prevention in the Process Industries*, vol. 57, pp. 94–100, 2018.

[23] Z. J. Su, S. Z. Du, H. X. Huang, and Z. B. Fan, "Numerical simulation analysis of deformation and damage of deep tunnel's surrounding rock," *The Chinese Journal of Geological Hazard and Control*, vol. 27, no. 2, pp. 121–126, 2016.

[24] Y. M. Zhao, "Numerical simulation study on the stability of surrounding rock of roadway with roadway section size," *Hydraulic Coal Mining & Pipeline Transportation*, vol. 3, pp. 24–26+29, 2018.

[25] X. Wang, Z. Wen, Y. Jiang, and H. Huang, "Experimental study on mechanical and acoustic emission characteristics of rock-like material under non-uniformly distributed loads," *Rock Mechanics and Rock Engineering*, vol. 51, no. 3, pp. 729–745, 2018.

[26] Q. Liu, J. Chai, S. Chen, D. Zhang, Q. Yuan, and S. Wang, "Monitoring and correction of the stress in an anchor bolt based on pulse pre pumped Brillouin optical time domain analysis," *Energy Science & Engineering*, vol. 8, no. 6, pp. 2011–2023, 2020.

[27] X. N. Chen, X. Y. Xiong, J. C. Wang, and P. Shen, "Numerical simulation study on asymmetric characteristics of surrounding rock stress in right angle trapezoidal roadway," *Coal Science and Technology*, vol. 47, no. 4, pp. 57–62, 2019.

[28] J. X. WU and S. L. Fang, "Mechanical mechanism and control technology of floor heave of high stress thick coal seam under dynamic pressure," *Coal Science and Technology*, vol. 46, no. 12, pp. 86–91, 2018.

[29] F. Chen, C. He, and J. H. Deng, "Concept of high geostress and its qualitative and quantitative definitions, rock and soil mechanics," *Rock and Soil Mechanics*, vol. 36, no. 4, pp. 971–980, 2015.

[30] C. D. Tian and H. B. Bai, "Impact analysis of roadway size and layout on stability of surrounding rock," *Safety in Coal Mines*, vol. 46, no. 8, pp. 220–223, 2015.

[31] K. Li, H. L. Gu, K. P. Qiu, and K. Q. Qi, "Numerical simulation analysis on influence of tunnel cross-section on stability of surrounding rock," *Coal Technology*, vol. 35, no. 3, pp. 52–54, 2016.

[32] Y. F. Sun, "Affects of in-situ horizontal stress on stability of surrounding rock roadway," *Journal of China Coal Society*, vol. 35, no. 6, pp. 891–895, 2010.

[33] W. S. Zhao, L. J. Han, Y. D. Zhang, Z. N. Zhao, and G. F. Wang, "Study on the influence of principal stress on the stability of surrounding rock in deep soft rock roadway," *Journal of Mining & Safety Engineering*, vol. 32, no. 3, pp. 504–510, 2015.

[34] Q. L. Liu, "Study on affecting of in-situ stress distribution law on stability of roadway surrounding rock," *Coal Technology*, vol. 34, no. 12, pp. 37–39, 2015.

[35] W. S. Zhao, L. J. Han, Z. N. Zhao et al., "Influence of principal stress on surrounding rock stability of roadway intersection," *Rock and Soil Mechanics*, vol. 36, no. 6, pp. 1752–1760, 2015.

[36] T. Liu and Z. Y. Li, "Study on influence of maximum horizontal stress on roadway stability," *Coal Technology*, vol. 37, no. 7, pp. 86–89, 2018.

[37] L. Zhu, "Research of deformation of roadway surrounding rock under effect of high horizontal stress in Gaojiapu coal mine," *Industry and Mine Automation*, vol. 43, no. 11, pp. 58–62, 2017.

[38] G. X. Xie, C. M. Li, and L. Wang, "Mechanical characteristics and practical application on stress shell of roadway surrounding rock," *Journal of China Coal Society*, vol. 41, no. 12, pp. 2986–2992, 2016.

[39] Z. H. Kan, "Study on the influence of the maximum horizontal principal stress on the stability of surrounding rock," *Mining Technology*, vol. 18, no. 3, pp. 40–42, 2018.

[40] W. J. Yu, G. S. Wu, and C. Yuan, "Engineering characteristics and stability of surrounding rock in deep high stress large deformation roadway," *Mineral Engineering Research*, vol. 32, no. 2, pp. 29–36, 2017.